Effect of Organophilic Montmorillonite on Polyurethane/montmorillonite Nanocomposites

Bing Han,[1] Aimin Cheng,[1] Gending Ji,[1] ShiShan Wu,[1] Jian Shen[1,2]

[1]*Research Center of Surface and Interface Chemistry and Engineering Technology, Nanjing University, Nanjing 210093, People's Republic of China*
[2]*College of Chemistry and Environment Science, Nanjing Normal University, Nanjing 210097, People's Republic of China*

Received 23 January 2003; accepted 2 May 2003

ABSTRACT: Different kinds of organophilic montmorillonite cotreated by cetyltrimethyl ammonium bromide (CTAB) and aminoundecanoic acid (AUA) were synthesized and applied to prepare polyurethane/montmorillonite nanocomposites via solution intercalation. The results of wide-angle X-ray diffraction (WAXD) and transmission electron microscopy showed that, for the montmorillonite modified with CTAB and CTAB/AUA (molar ratio of 1/2), an ordered intercalated nanostructure was derived, while for the montmorillonite treated with AUA, a disordered nanostructure was derived. The tensile properties of the polyurethane (PU) nanocomposites showed higher enhancement relative to PU matrix. TG showed that there is some enhancement in degradation behavior between the nanocomposites and PU matrix. DMTA results showed that nanocomposites from some organophilic montmorillonites showed a much higher storage modulus below and above glass transition temperature, while the nanocomposites from montmorillonite treated by AUA show an even lower storage modulus. The loss curves showed that the main glass transition temperature of PU was improved to some extent for the nanocomposites. The water absorption of PU and nanocomposites was also studied and the difference in reduction was thoroughly analyzed. © 2003 Wiley Periodicals, Inc. J Appl Polym Sci 91: 2536–2542, 2004

Key words: polyurethanes; montmorillonite; nanocomposites; solution intercalation; TEM

INTRODUCTION

Polyurethane (PU) is a versatile engineering material because it has excellent abrasion resistance and displays properties of both plastics and elastomers.[1,2] Conventional PU, however, cannot meet the demand of application for its poor thermal and mechanical properties.[3] The modification of PU with fillers is always applied to improve its overall properties, among which is the use of organophilic montmorillonite (MMT) to achieve nanocomposites.[4–6] In general, because of the ultrafine phase dimensions involved, nanocomposites always exhibit new and improved properties in comparison with their microcomposite or macrocomposite counterparts.[7–9] Now, many researchers have reported the synthesis of PU/MMT nanocomposites through various routines, while most of them are focused on the preparation and properties of the nanocomposites,[10–13] no systematic work was done to study the effect of organophilic montmorillonite with different polarity on properties of PU/MMT nanocomposites.

Correspondence to J. Chen (shenjian@nju.edu.cn).

Journal of Applied Polymer Science, Vol. 91, 2536–2542 (2004)

In this paper, different kinds of organophilic montmorillonite cotreated by cetyltrimethyl ammonium bromide (CTAB) and aminoundecanoic acid (AUA) were synthesized and applied to prepare PU/MMT nanocomposites via solution intercalation. The nanocomposites prepared were characterized by wide-angle X-ray diffraction (WAXD) and transmission electron microscopy (TEM). The effect of organophilic montmorillonites on properties of PU/MMT nanocomposites, such as dispersion in PU matrix, thermal properties, mechanical properties, and water absorption, was also studied and analyzed. The result is illuminating for the preparation of polymer/MMT nanocomposites.

EXPERIMENTAL

Materials

The source Ca-montmorillonite (Ca-MMT) with a cation-exchange capacity (CEC) of 110 meq/100 g was purified and screened by a 325-mesh sieve and then was completely dried at 120°C *in vacuo* for 24 h before use. 4,4′-Diphenylmethylate diisocyanate (MDI) was purchased from Huntsman and was used without further purification. Poly(propylene glycol) (PPG, M_w = 2000) was donated by Arch Chemicals and was dehydrated by coboiling with toluene for 2.5 h. Dim-

ethylforamide (DMF) and 1,4-butanediol (1,4-BD) were dried over molecular sieves before use and then were distilled *in vacuo* for further purification. Common reagents were used without further purification.

Preparation of polyurethane

Polyurethane was prepared with the molar ratio of 3/1/2 (MDI/PPG/1,4-BD) via bulk polymerization. A defined amount of MDI was put into a fully dried reaction vessel and then was heated to 70°C to melt before the addition of stoichiometric PPG. The system was kept in 80°C for 2.5 h at dry N_2 atmosphere to get prepolymer. The prepolymer then was cooled to 40°C and stoichiometric 1,4-BD was added to it. After 1 min of vigorous stirring, the system was degassed fully *in vacuo* and then was cast into a mold. After 16 h of reaction at 120°C, the PU was attained.

Preparation of organophilic MMT and nanocomposites[14]

Ca-MMT (120 g) was dispersed in 1,200 mL of distilled water by violent stirring at 80°C and the MMT dispersion was derived; slightly excessive amounts of CTAB and AUA with molar ratio of 1/2, acidified by an appropriate amount of concentrated hydrochloric acid, were dispersed into 600 mL alcohol and 600 mL distilled water separately, and the solutions were called CTAB alcoholic solution and AUA aqueous solution, respectively. The latter two then were added to the MMT dispersion and the resultant suspension was vigorously stirred for another 8 h at 80°C. The cotreated MMT was repeatedly washed by alcohol and distilled water at 50°C until no AgCl precipitate occurred at room temperature when the filtrates were titrated with 0.1*N* $AgNO_3$. The filtered cakes were then dried *in vacuo* at 80°C for 12 h. The dried cakes were ground and screened with a 325-mesh sieve to obtain the cotreated MMTs and were termed M12. The organophilic MMTs monotreated by CTAB or AUA was prepared as widely described and were termed M10 and M01 here. All the dried organophilic MMT were kept in a sealed desiccator ready for further experiments.

O-MMT (0.15 g) was dispersed into 25 g DMF by supersonic dispersion for 15 min before the addition of 2.85 g of PU. The system was vigorously stirred at room temperature until polyurethane was dissolved. After another 15 min of supersonic dispersion, the suspension was put quietly for a few minutes to degas, and then was cast into a polytetrafluoroethylene mold. A membrane was obtained at 70°C and then dried at 80°C *in vacuo* for 24 h. The PU matrix membrane was made as above except that no O-MMT was added. All the membranes prepared were kept in a sealed desiccator before the following experiments.

Characterization and test

FTIR of the pristine and organophilic MMT was conducted on a VECTOR 22 IR analyzer. WAXD characterization of pristine Ca-MMT and organophilic MMT was made directly from their powder. The dispersibility of MMT in PU matrix was evaluated with X-ray diffractometer measurements carried out on nanocomposites films. All of the WAXD measurements were carried out with a SHIMADZU XRD-6000 with CuKα radiation (0.154 nm). The morphology of PU/MMT was imaged using a JEM-200 CX TEM. Ultrathin sections (20 nm) were cut from nanocomposites films cured in epoxy capsules using a Reichert-Jung Ultracut E microtome.

Tensile and tear tests were done using an Instron-4466 at a crosshead speed of 500 mm/min. The result reflects an average of five specimens and all the mechanical properties were tested at 23°C. The thermogravimetric analysis was done on a TA 2100-SDT 2960 with the temperature ramp of 10°C/min under N_2 atmosphere. The dynamic mechanical thermal analysis was carried out on a Rheometric Scientific DMTA V in the tension mode using rectangular samples. A frequency of 10 Hz,and a static force of 0.1 N were used. The temperature ramp was 3.0°C/min and the scanning range was from –100 to 80°C.

The water absorption test was carried out referring to the specifications of ASTM D570, and the test specimens were cut in the shape of $12.5 \times 4.0 \times 0.145$ mm^3. The totally dried specimens were weighed to the nearest 0.0001 g to get the initial weight, W_0. The conditioned specimens were entirely immersed in a container of deionized water maintained at 25 $\pm$ 0.2°C for a definite interval. After a definite interval, the specimens were removed from the water, one at a time, surface water on specimens was removed with a dry cloth, and the specimens were weighed immediately to get the weight, W_1. The percentage of increase in weight of the samples was calculated to the nearest 0.1% by using the formula $(W_1 - W_0)/W_0$.[15]

RESULTS AND DISCUSSION

Cotreated MMT

In the present work, CTAB and AUA are applied to cotreat MMT with the molar ratio of 1/0, 1/2 and 0/1, and the cotreated MMTs are termed M10, M12, and M01, respectively. To testify to the effect of modification, the FTIR spectra of pristine and treated MMTs are shown in Figure 1.

In the spectra, the peaks at 2,922 cm^{-1} and 2,854 cm^{-1} contribute to the absorbance of methylene's

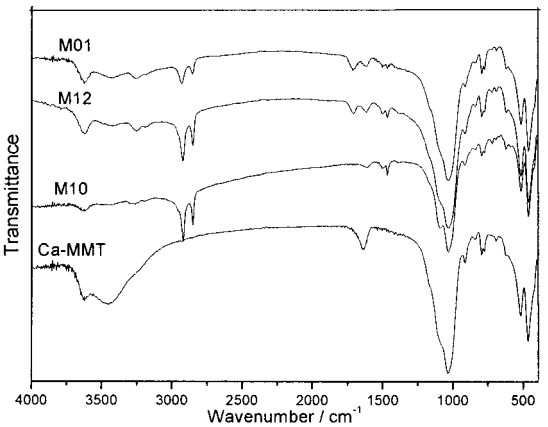

Figure 1 FTIR of the pristine and organophilic MMTs.

asymmetric and symmetric stretching vibrations, the absorbance at 1,470 cm^{-1} belongs to methylene's bending vibration, the peak at 1,715 cm^{-1} corresponds to absorbance of carbonyl stretching vibration, which means after treatment, CTAB has been successfully tethered to the surface of the platelet in M10 and M12, and AUA has been tethered to the surface of the platelet in M12 and M01. The accurate ratio of CTAB to AUA in M12 is greatly influenced by the procedure and is not determined here.

For detecting the interlayer heights before and after treatment, the WAXD spectra of the pristine and treated MMT are depicted in Figure 2.

The d-spacings of the MMT before and after treatment are calculated using Bragg's relation according to the angle of the 001 diffraction peak in the WAXD pattern. $2d\sin\theta = \lambda$, where λ corresponds to the wave length of the X-ray radiation used in the diffraction experiment, d to the spacing between diffractional lattice planes, and θ is the measured half diffraction angle or glancing angle.[16] It can be concluded that, after treatment, the d001s have increased from 1.54 nm of pristine MMT to 1.77 nm for M01, 1.96 nm for M12, and 2.05 nm for M10. The exchange of Ca^{2+} to quats expands the interlayer space greatly. The d001 of M10 is a little larger than that of M12 and M01, which is because the molecule chain of AUA is a little shorter.

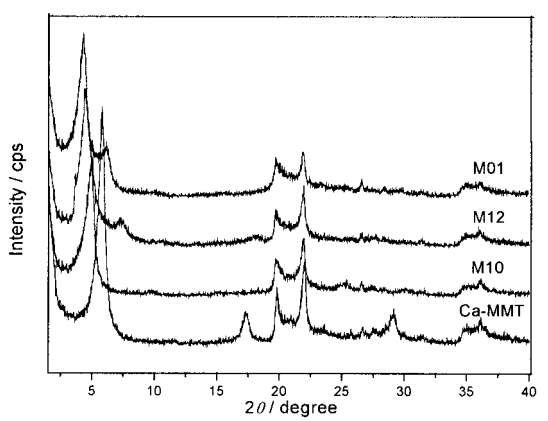

Figure 2 WAXD of the pristine and organophilic MMTs.

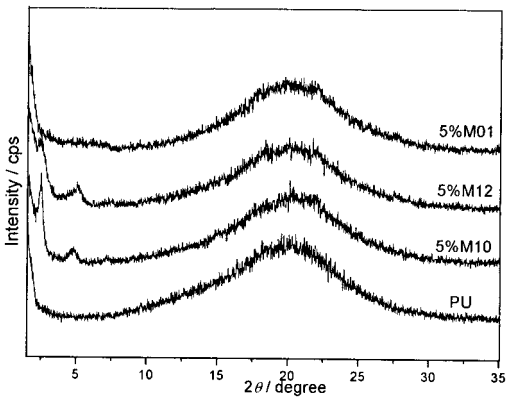

Figure 3 WAXD of PU and PU/MMT nanocomposites from cotreated MMTs: 5%M01, nanocomposites containing 5% M01; 5%M12, nanocomposites containing 5% M12; 5%M10, nanocomposites containing 5% M10; PU, pure polyurethane.

Characterization of PU/MMT nanocomposites

In this paper, the PU/MMT nanocomposites membranes were testified by WAXD from 1.5 to 35° and the result is depicted in Figure 3. From Figure 3, it can be seen that the nanocomposites from M10 and M12 show a diffraction peak at 2.55°, which means an ordered intercalation structure was obtained, while the nanocomposites from M01 show no diffraction peak from 1.5 to 10°, which means a disordered exfoliated structure was derived,[17] although M01 presents the minimum interlayer space. So it can be concluded that M01 is more compatible with PU prepared relative to M10 and M12. As reported by other researchers,[18] the MMT modified by polar surfactants should show more polarity and can provide more favorable interactions between the MMT and the polar polymer (e.g., PU). For further characterization, TEM was applied to study the nanostructure morphology of the nanocomposites from M10 and M01. The result is shown in Figure 4.

From the WAXD conclusion above, the interlayer space of MMT should be more than 5.80 nm for PU/MMT with M01, and should be about 3.46 nm for that with M10. In Figure 4(a), it can be seen that the clay layers are dispersed homogeneously and most of them showed ordered structure with the interlayer space of about 4 nm, which declared the formation of an ordered intercalation nanostructure, while for Figure 4(b), the clay interlayer space is much larger, about 8 nm, which is strong evidence for the formation of an

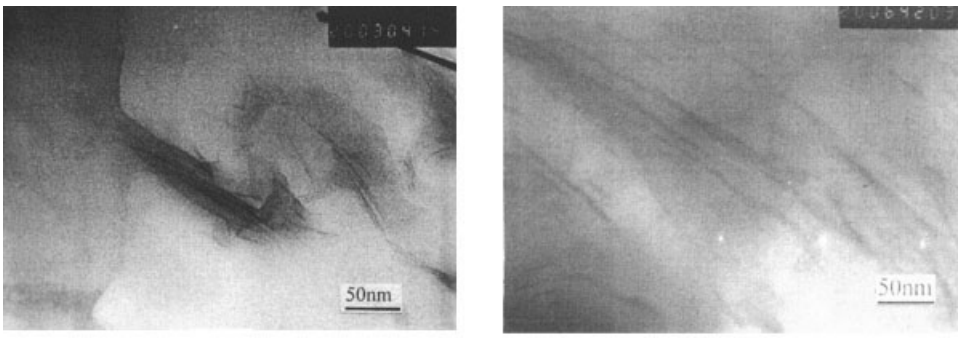

Figure 4 TEM of the PU/MMT nanocomposites at the loading of 5%: (a) PU/MMT from M10; (b) PU/MMT from M01.

exfoliation structure.[15] This result is consistent with the conclusion from WAXD. It can be concluded that, relative to M10 and M12, M01 has much stronger intercalating power.

From the WAXD of Figure 3, it can also be seen that, compared with the PU matrix, all the nanocomposites show a diffraction peak at about 20.4°,[19] especially for the nanocomposites from M12, which means the introduction of clay layers induced the crystallization of PU hard segments. This change of crystallization may lead to some change of mechanical properties. In this paper, it was thought that there should be two competitive factors dominating the crystallinization of the nanocomposites. One is the inducing effect of MMT layers, the other is the inhibition effect of MMT layers on the crystallization of PU. Relative to M10 and M01, M12 shows much stronger inducing effect, while for the totally exfoliated and intercalated structure, the inducing effect is much weaker and the inhibition effect is dominant. So the nanocomposites from them show less crystallinity.

Thermal properties

As reported by many other researchers, the introduction of MMT layers can greatly improve the thermal properties of the polymer matrix.[16] In our research, the thermogravimetric analysis of the PU/MMT nanocomposites was carried out. It was found that all of the specimens displayed two obvious degradation processes from room temperature to 600°C. To study the degradation thoroughly, the onset temperature (T_d) of the two degradation processes and the respective temperature of maximum degradation rate (DTG_{max}) were derived and are shown in Table I.

From Table I, it can be seen that, relative to PU matrix, the first onset temperature (T_{d1}) of the nanocomposites from M10 and M12 is higher while that of the nanocomposites from M01 shows a little decrease. But the latter shows the maximum $DTG1_{max}$. As to T_{d2} and $DTG2_{max}$, all the nanocomposites show some increase compared with PU matrix. From the table, it can also be seen that, relative to the other two nanocomposites, the nanocomposites from M12 exhibit the greatest increase, which may correspond to the result of WAXD. In our opinion, the first degradation process corresponds to the release of the little molecules or unstable side chains, which will degrade at lower temperature. The introduction of a little well-dispersed MMT can prevent the heat transport and then improve the thermal stability of the nanocomposites.[20] But because the O-MMT itself contains some low molecules that will release at lower temperature,[14] too many of them are sure to impair the thermal stability of the nanocomposites. As to DTG2, the degradation of the PU molecular backbone is dominant, the introduction of MMT limits the motion of PU molecule, and then leads the nanocomposites to exhibit higher enhancement.

The dynamic mechanical thermal analysis is a good method to study relaxation behavior and to detect the change in loss (or T_g, glass transition temperature) and storage modulus. In this paper, the PU matrix and the nanocomposites from all cotreated MMTs were ap-

TABLE I
Thermogravimetric Analysis Results of PU and PU/MMT Nanocomposites

	O-MMT	O-MMT content (%)	T_{d1} / °C	T_{d2} / °C	$DTG1_{max}$ / °C	$DTG2_{max}$ / °C
1	PU	0	294.77	373.00	313.74	394.62
2	M10	5%	300.72	378.14	326.85	397.74
3	M12	5%	300.05	387.37	329.45	402.49
4	M01	5%	286.75	380.86	333.06	401.4

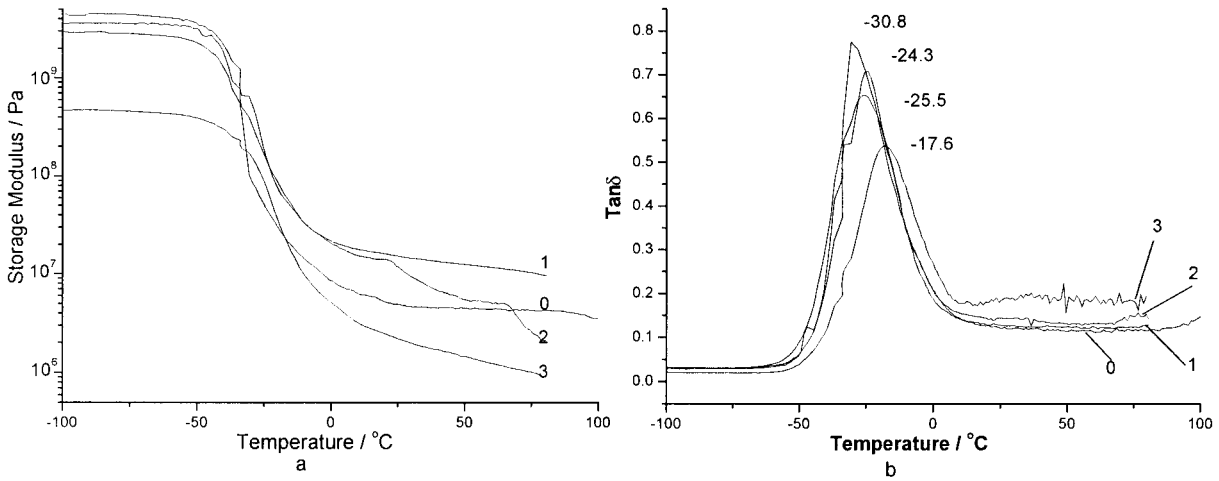

Figure 5 DMTA results of PU and PU/MMT nanocomposites: (a) storage modulus; (b) tanδ. 0, PU matrix; 1, nanocomposites containing 5% M10; 2, nanocomposites containing 5% M12; 3, nanocomposites containing 5% M01.

plied to carry out this research and the results are derived as shown in Figure 5.

From Figure 5(a), it can be concluded that, relative to PU matrix, the nanocomposites from M12 and M10 show a higher storage modulus before and after glass transition, which is consistent with the conclusion above. But the nanocomposites from M01 show a very low storage modulus compared with the other nanocomposites and even the PU matrix, which is unexplainable now. From the result of WAXD, it has been concluded that the hard segments of the nanocomposites from M12 show more crystallinity, which is reflected in Figure 5(a). At about 23°C and about 66°C there are two steep drops in the curve of M12, while only slightly decreasing behavior can be observed for the other nanocomposites and the PU matrix. This is because the nanocomposites from M12 have more crystalline domains, with the increase of the temperature, the disordering of the crystalline domains produces a strong modulus reduction above the melting. In this paper, the hard segment ratio of the PU prepared is very low. As reported by other researchers, the PU with low hard segment ratio is more favorable for the intercalation.[19] The hard segment will crystalline in PU matix; as to the two steep drops, it is thought in this paper that the first drop is contributed to by the free hard segment, which will relax at low temperature, and the second drop at 66°C should correspond to the relaxation of the hard segments restricted by the MMT interlayers. From the curve of the nanocomposites from M01, it can also be seen that the curve keeps steep decreasing behavior relative to the others. In the WAXD, it has been testified that it should have exfoliated structure while the others only show characteristics of intercalated structure. The exfoliated layers have two competitive effects on the crystallization of the PU. One is the inducing effect of the clay layers, the other is the inhibiting effect of the overdispersed clay layers. When the clay layers are delaminated, the exfoliated layers strongly inhibit the crystallization of PU hard segments, and the inhibiting effect becomes dominant. So more small crystal was formed, which will be disturbed at lower temperature. So the nanocomposites from M12 show very steep decreasing behavior above glass transition. This explanation also applies to the behavior of the nanocomposites from M10, which also show steeper decreasing behavior relative to the amorphous PU matrix.

As to the loss curves, tanδ in Figure 5(b), at about –30 to −16°C, an intense peak, due to the mobilization of the amorphous soft domains, appears in the correspondence of the main storage modulus drop. This suggests that this peak is associated to the main glass transition of the system,[20] due to the amorphous domains. It can be seen that the glass transition temperature was improved from –30.8°C of PU matrix to −25.5°C of nanocomposites from M12, −24.3°C of nanocomposites from M10, and −17.6°C of nanocomposites of M01. This improvement corresponds to the restriction of the soft segments of PU. The nanocomposites from M01 have the maximum interfacial interaction area due to its exfoliated nanostructure, and then the strongest restriction effect, so the largest improvement was derived. As the reflection of Figure 5(a), a loss peak at about 36°C was observed in the correspondence of the steep drop in the modulus curve of the nanocomposites from M01. No obvious peak was detected for the other nanocomposites and the PU matrix which corresponds to the disordering of the crystalline domains. Owing to the low ratio of hard segment in the PU matrix prepared in this paper, no obvious secondary relaxation peak was observed between –95 and −70°C, which has been reported.[20]

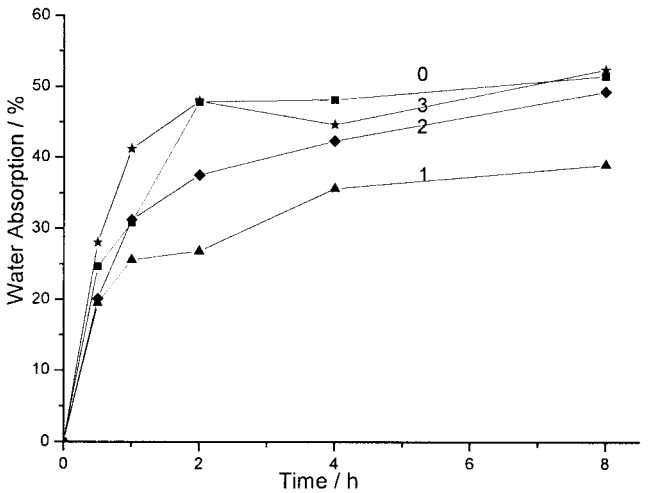

Figure 6 Water absorption curve of PU and PU/MMT nanocomposites. 0, PU matrix; 1, nanocomposites containing 5% M10; 2, nanocomposites containing 5% M12; 3, nanocomposites containing 5% M01.

This result is consistent with the reports by many other researchers who reported the introduction of MMT layers can also improve the glass transition temperature greatly.[12]

Water absorption

Properties of many materials change with the difference in water absorption. As to PU elastomer, its water absorption greatly influences its stability in actual application. Its properties, mainly mechanical properties, decrease greatly with the increase of water absorption. So it is important to study the change of moisture adsorption before and after modification. In this paper, owing to the limits of specimen preparation, this measurement was carried out referring to the corresponding ASTM specifications, and the result only displayed some qualitative trend. The result is shown in Figure 6.

Originally, PU is hydrophilic and O-MMT is organophilic or hydrophilic according to the difference of surfactants. From Figure 6, it can be found that, at the first stage, PU matrix and the nanocomposites from M01 and M12 show a much higher water absorption rate, and they attain the balance of water absorption much quicker relative to the nanocomposites from M10. The introduction of MMT layers increases the path for water molecules to penetrate the nanocomposites film and then delays the time to attain balance. On the other hand, the existence of organophilic MMT also decreases the total water absorption accordingly. In this paper, M01 is hydrophilic owing to the hydrophilic AUA, and M10 is more organophilic owing to CTAB; M12 is both organophilic and hydrophilic. Compared with PU matrix, the nanocomposites from M01 have approximately equal water absorption while they may take more time to attain the balance. The nanocomposites from M10 have the minimum water absorption and take the longest time to attain the balance. The result is consistent with the nature of the surfactants applied to modify the MMT. Decrease of water absorption means the material has more stable properties, which is interesting for practical applications.

Mechanical properties

The tensile and tear properties of the PU matrix and PU/MMT nanocomposites membrane are demonstrated in Table II.

It can be seen that, relative to the PU matrix, all of the nanocomposites show high enhancement in tensile and tear properties. Compared with the PU matrix, the nanocomposites from M12 show the highest strength, enhanced by about 42%, although the nanocomposites from M01 show an exfoliated structure, which may be relative to the difference of crystallinity of the nanocomposites. The nanocomposites from M12 have more crystallinity, which can act as physical crosslinking position, which then results in higher enhancement. For Table II, it can also be seen that, although the strength was greatly improved, the elongation at break also shows a definite improvement, especially for the nanocomposites from M12 and M01; the elongation was enhanced by about 30 and 50%, which means the MMT layers toughened the PU matrix, which is different with the previous report of other polymers.[7]

TABLE II
Mechanical Properties of PU and PU/MMT Nanocomposites

	O-MMT	Concentration (%)	Tensile strength (MPa)	Tensile modulus (MPa)	Elongation at break (%)	Tear strength (MPa)
0			10.6	5.1	1090	2.8
1	CTAB	5	14.6	7.1	1510	3.6
2	1/2	5	15.0	7.1	1470	3.7
3	AUA	5	13.9	7.0	1630	3.9

The authors are thankful for the partial financial support from Analysis and Testing Foundation of Nanjing University. Many thanks to the help of Ms. Yuan Zuanru with the DMTA measurements and the help of Mr. Hong Jianming with the TEM characterization.

References

1. Woods, G. The ICI Polyurethane Book; Wiley: Chichester, 1990; Chapter 1.
2. Comstock, M. T. Urethane Chemistry and Applications; ACS Symposium Series 172; Am Chem Soc: Washington, DC, 1981; Chapter 1.
3. Fabris, H. T. Advances in Urethane Science and Technology; Technomic: New York, 1976.
4. Alexandre, M.; Dubois, P. Mater Sci Eng R Rep 2000, 28, 1.
5. Chang, J. H.; An, Y.; J Polym Sci Part B Polym Phys 2002, 40, 670.
6. Tien, Y.; Wei, K. H. Macromolecules 2001, 34, 9045.
7. Okada, A.; Kawasumi, M. Polym Prepr 1987, 28, 447.
8. Lan, T.; Pinnavaia, T. J. Chem Mater 1994, 6, 2216.
9. Yano, K.; Usuki, A.; Okada, A. J Polym Sci Part A Polym Chem 1993, 31, 2493.
10. Yao, K. J.; Song, M.; Hourston, D. J. Polymer 2002, 43, 1017.
11. Li, X. C.; Kang, T. Y.; Cho, W. J. Macromol Rapid Commun 2001, 22, 1306.
12. Ma, J. S.; Zhang, S. F.; Qi, Z. N. J Appl Polym Sci 2001, 82, 1444.
13. Hu, Y.; Song, L.; Xu, J. Colloid Polym Sci 2001, 279, 819.
14. Han, B.; Ji, G. D. Eur Polym J 2003, 39, 1641.
15. Chen, T. K.; Tien, Y. I.; Wei, K. H. Polymer 2000, 41, 1345.
16. Vaia, K. H.; Giannelis, E. P. Macromolecules 1997, 30, 8000.
17. Vaia, R. A.; Giannelis, E. P. Macromolecules 1997, 30, 7990.
18. Tanaka, G.; Goettler, L. A. Polymer 2002, 43, 541.
19. Tien, Y.; Wei, K. H. Polymer 2001, 42, 3213.
20. Tortora, M.; Gorrasi, G.; et al. Polymer 2002, 43, 6147.